

Atomic transfer in halogen-bonded complexes mediated by polarizing environments: Mimicking intra- and inter-molecular effects in a series of cocrystals of N-bromosaccharin with pyridines

Emmanuel Aubert,^a Irène Nicolas,^b Olivier Jeannin,^b Marc Fourmigué^{b,*} and Enrique Espinosa,^{a,*}

^a *Laboratoire CRM2, UMR CNRS 7036, Institut Jean Barriol, Université de Lorraine, BP 70239, 54506 Vandoeuvre-les-Nancy (France)*

^b *Univ Rennes, CNRS, ISCR (Institut des Sciences Chimiques de Rennes), UMR 6226, 35000 Rennes (France)*

SUPPLEMENTARY INFORMATION

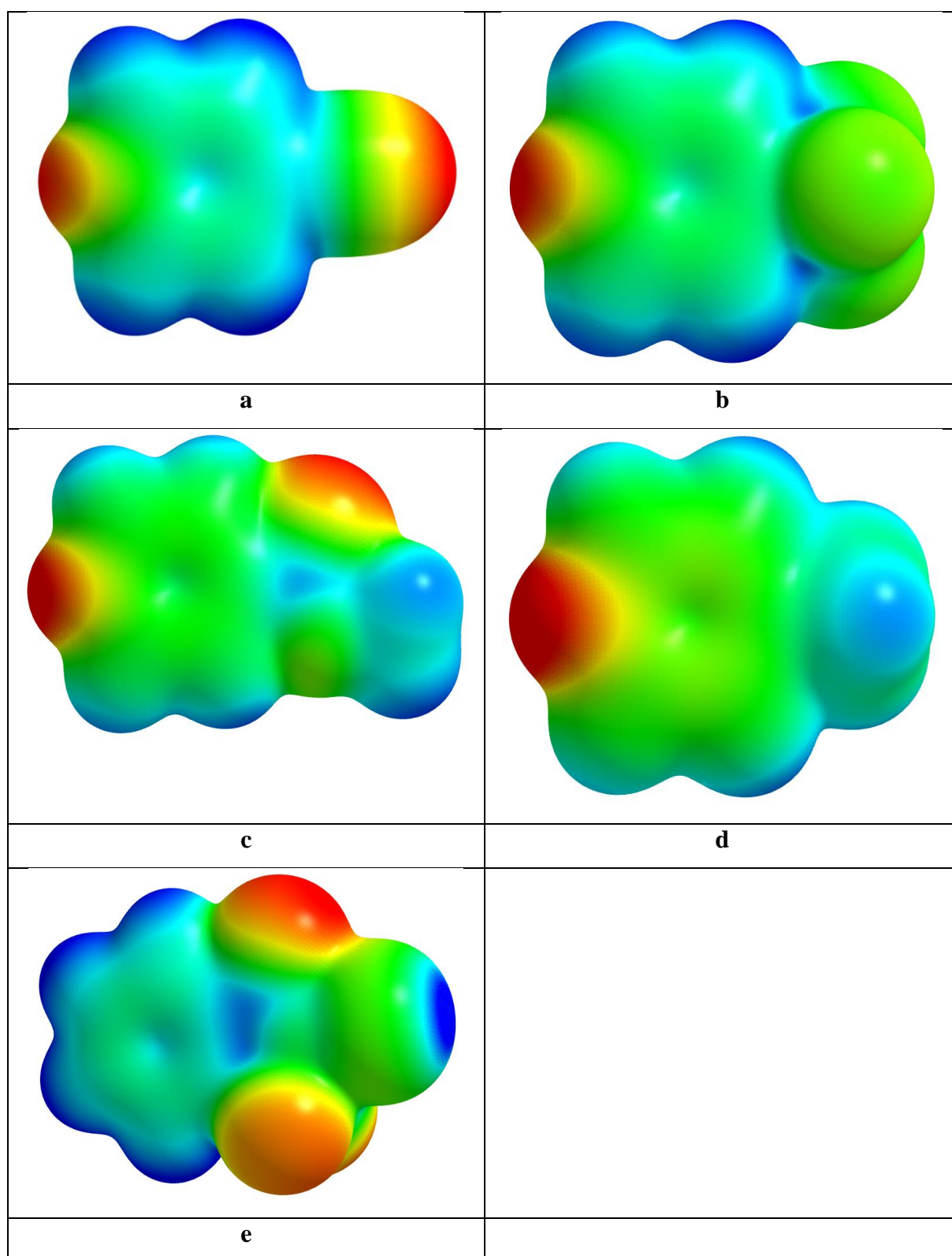


Figure S1. MESP on $\rho = 0.002$ a.u. (from -0.05 a.u. red to $+0.05$ a.u. blue) for the four XB acceptors **(a)** PyCN, **(b)** PyCF₃, **(c)** PyCO₂Me, **(d)** PyMe and **(e)** the XB donor NBrSac.

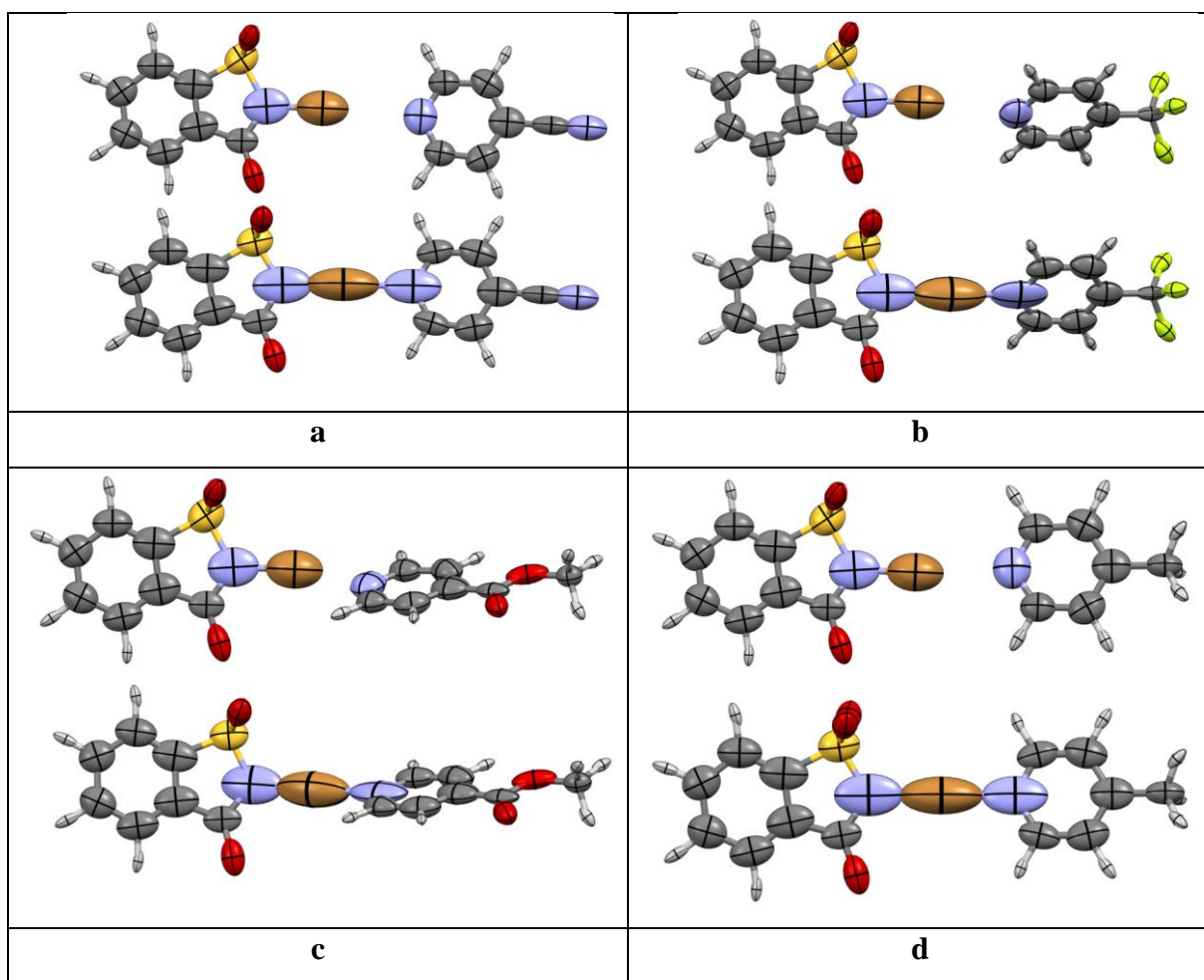


Figure S2. Polarizabilities for the four XB-adducts with the corresponding NBrSac donor and pyridines alone (a) NBrSac•••PyCN, (b) NBrSac•••PyCF₃, (c) NBrSac•••PyCO₂Me and (d) NBrSac•••PyMe.

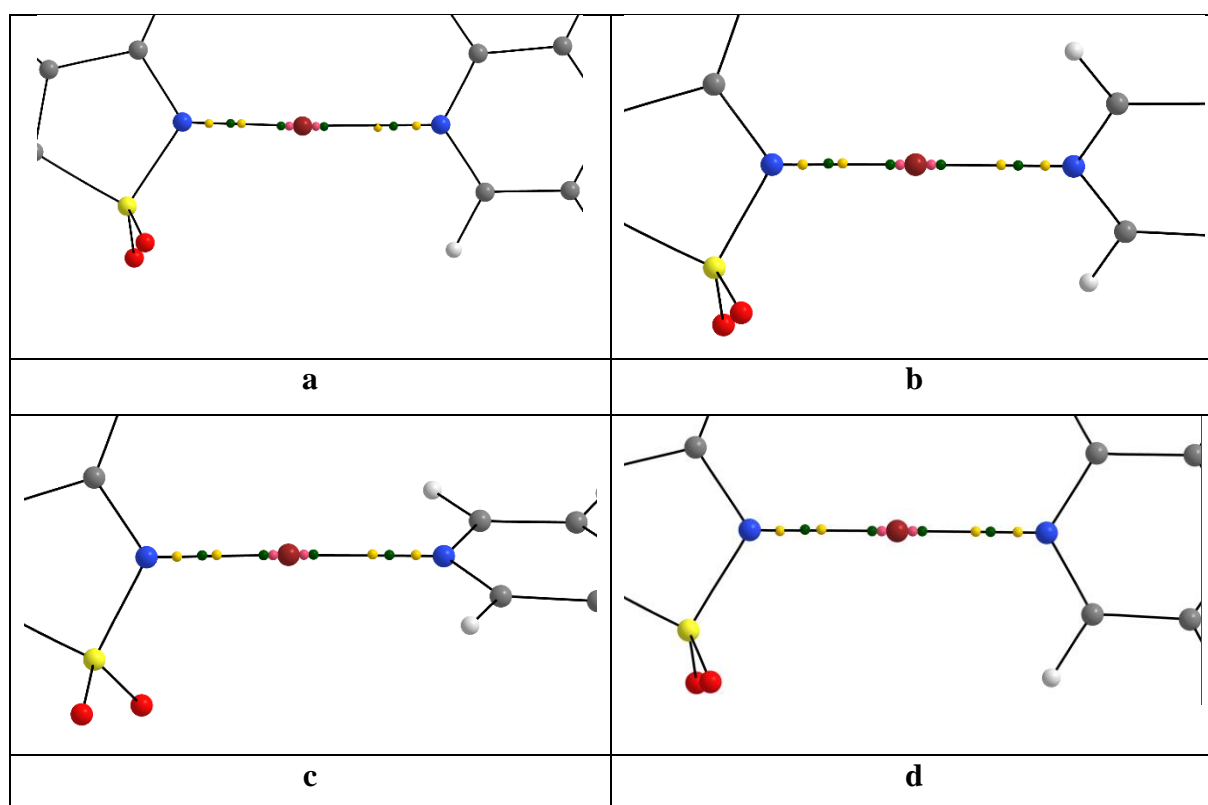


Figure S3. $(3,-3)$ (yellow) and $(3,-1)$ (green) and $(3,+1)$ (pink) critical points of the L -function along the halogen bonding motif $N_{\text{Sac}} \cdots \text{Br} \cdots N_{\text{Py}}$ of (a) $N\text{BrSac} \cdots \text{PyCN}$, (b) $N\text{BrSac} \cdots \text{PyCF}_3$, and (c) $N\text{BrSac} \cdots \text{PyCO}_2\text{Me}$ and (d) $N\text{BrSac} \cdots \text{PyMe}$, at experimental geometries

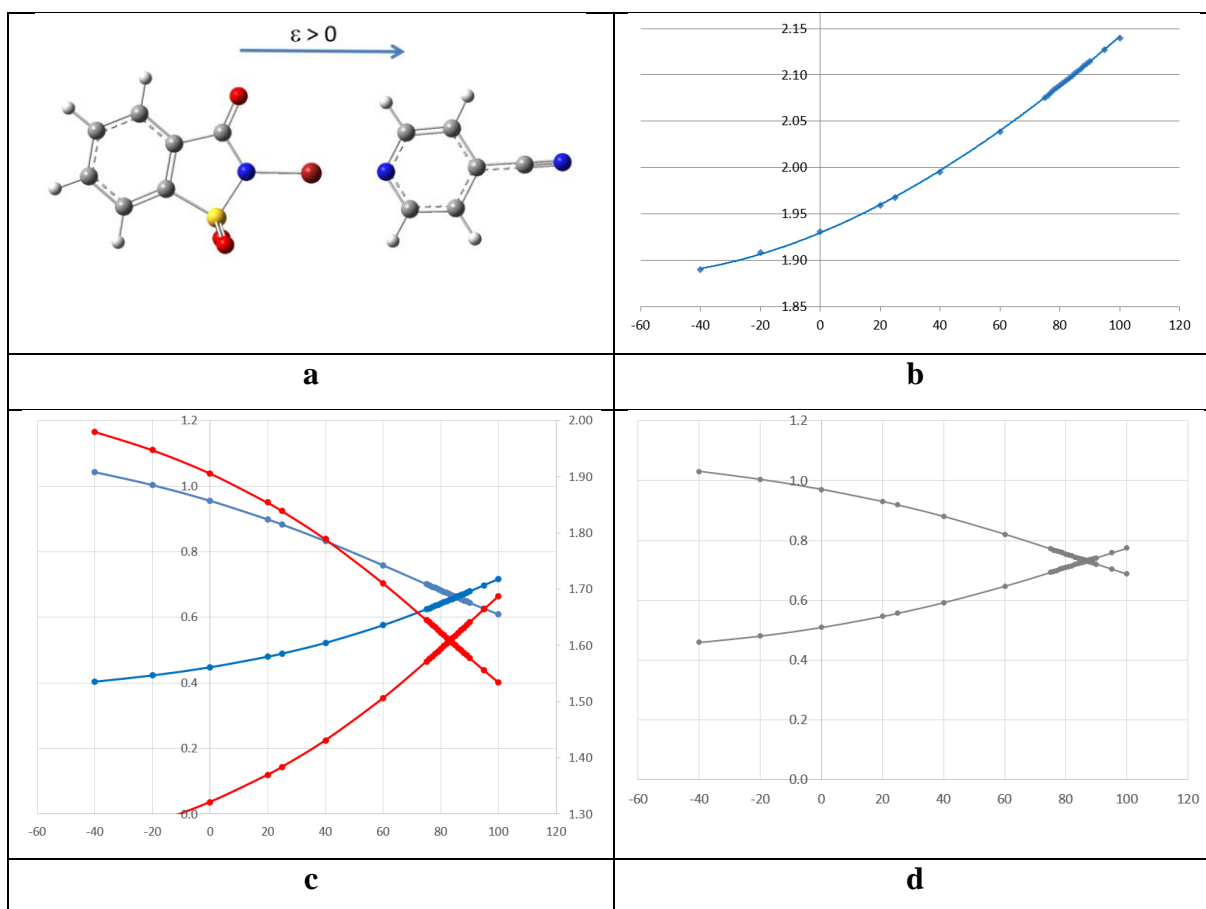


Figure S4. (a) NBrSac...PyCN adduct frozen at the experimental geometry (H atoms normalized at standard neutron distances) except for the Br-atom position, which has been optimized upon the application of an external electric field ϵ ranging $-40 < \epsilon < 100$ ($\times 10^{-4}$ a.u.), (b) $d(\text{NSac}\cdots\text{Br})$ (Å) vs ϵ ($\times 10^{-4}$ a.u.), the depicted fitting function is $d(\text{NSac}\cdots\text{Br}) = -1 \cdot 10^{-8} \cdot \epsilon^3 + 9 \cdot 10^{-6} \cdot \epsilon^2 + 1.3 \cdot 10^{-3} \cdot \epsilon + 1.9296$ (correlation factor $R^2 = 0.9999$). The corresponding ϵ vs $d(\text{NSac}\cdots\text{Br})$ curve leads to the fitting function $\epsilon = 6412.8 \cdot d^3 - 40017.0 \cdot d^2 + 83614.5 \cdot d - 58420.6$ (correlation factor $R^2 = 0.99999$), (c) ρ (blue curves and left scale in $\text{e}\text{\AA}^{-3}$) and $|V|/G$ (red curves and right scale dimensionless) at $\text{NSac}\cdots\text{Br}/\text{Br}\cdots\text{N}_{\text{Py}}$ BCPs (decreasing/increasing curves), and (d) DI vs ϵ for $\text{NSac}\cdots\text{Br}/\text{Br}\cdots\text{N}_{\text{Py}}$ interactions (decreasing/increasing curves). In (c) and (d), depicted curves are plotted for guiding eyes.

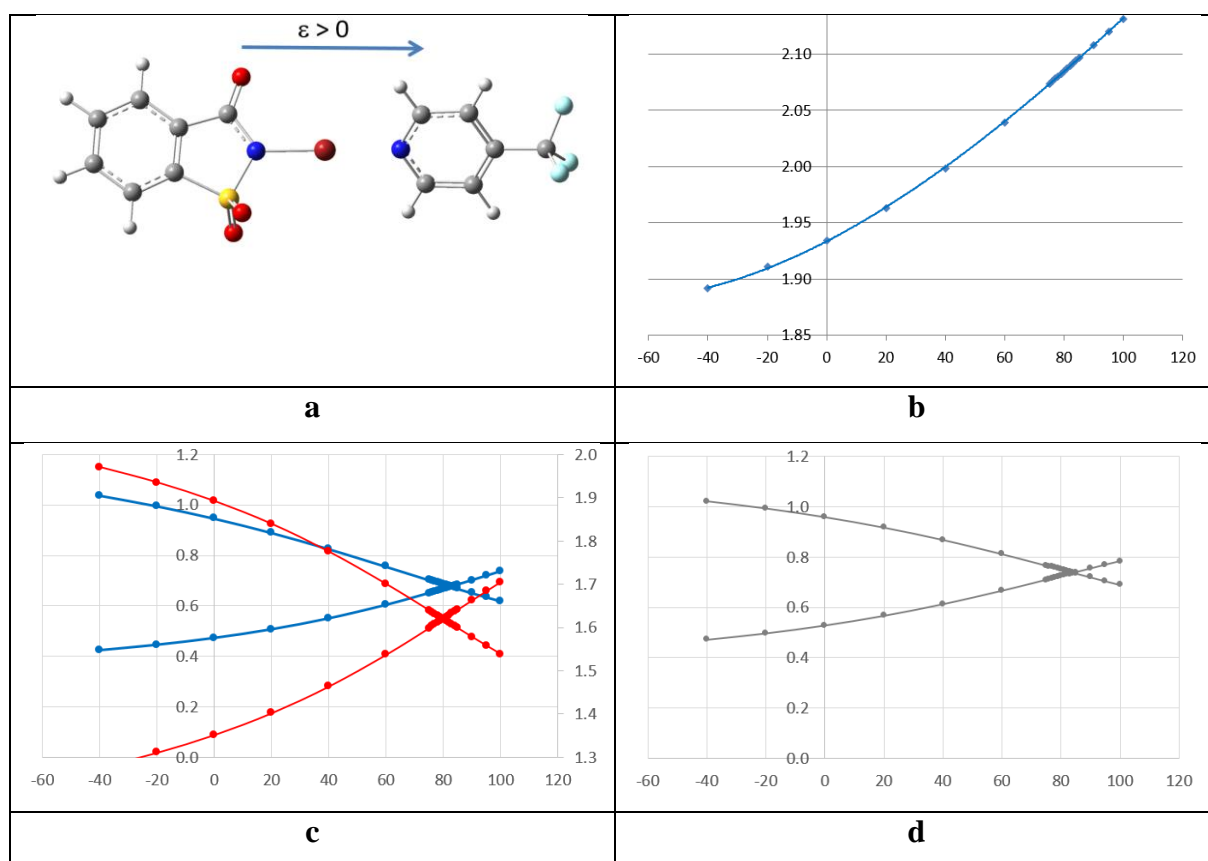


Figure S5. (a) NBrSac...PyCF₃ adduct frozen at the experimental geometry (H atoms normalized at standard neutron distances) except for the Br-atom position, which has been optimized upon the application of an external electric field ε ranging $-40 < \varepsilon < 100$ ($\times 10^{-4}$ a.u.), (b) $d(\text{N}_{\text{Sac}} \cdots \text{Br})$ (\AA) vs ε ($\times 10^{-4}$ a.u.), the depicted fitting function is $d(\text{N}_{\text{Sac}} \cdots \text{Br}) = -2 \cdot 10^{-8} \cdot \varepsilon^3 + 8 \cdot 10^{-6} \cdot \varepsilon^2 + 1.4 \cdot 10^{-3} \cdot \varepsilon + 1.9336$ (correlation factor $R^2 = 0.9999$). The corresponding ε vs $d(\text{N}_{\text{Sac}} \cdots \text{Br})$ curve leads to the fitting function $\varepsilon = 6200.9 \cdot d^3 - 38583.5 \cdot d^2 + 80447.1 \cdot d - 56125.7$ (correlation factor $R^2 = 0.99999$), (c) ρ (blue curves and left scale in $\text{e}\text{\AA}^{-3}$) and $|V|/G$ (red curves and right scale dimensionless) at $\text{N}_{\text{Sac}} \cdots \text{Br}/\text{Br} \cdots \text{N}_{\text{Py}}$ BCPs (decreasing/increasing curves), and (d) DI vs ε for $\text{N}_{\text{Sac}} \cdots \text{Br}/\text{Br} \cdots \text{N}_{\text{Py}}$ interactions (decreasing/increasing curves). In (c) and (d), depicted curves are plotted for guiding eyes.

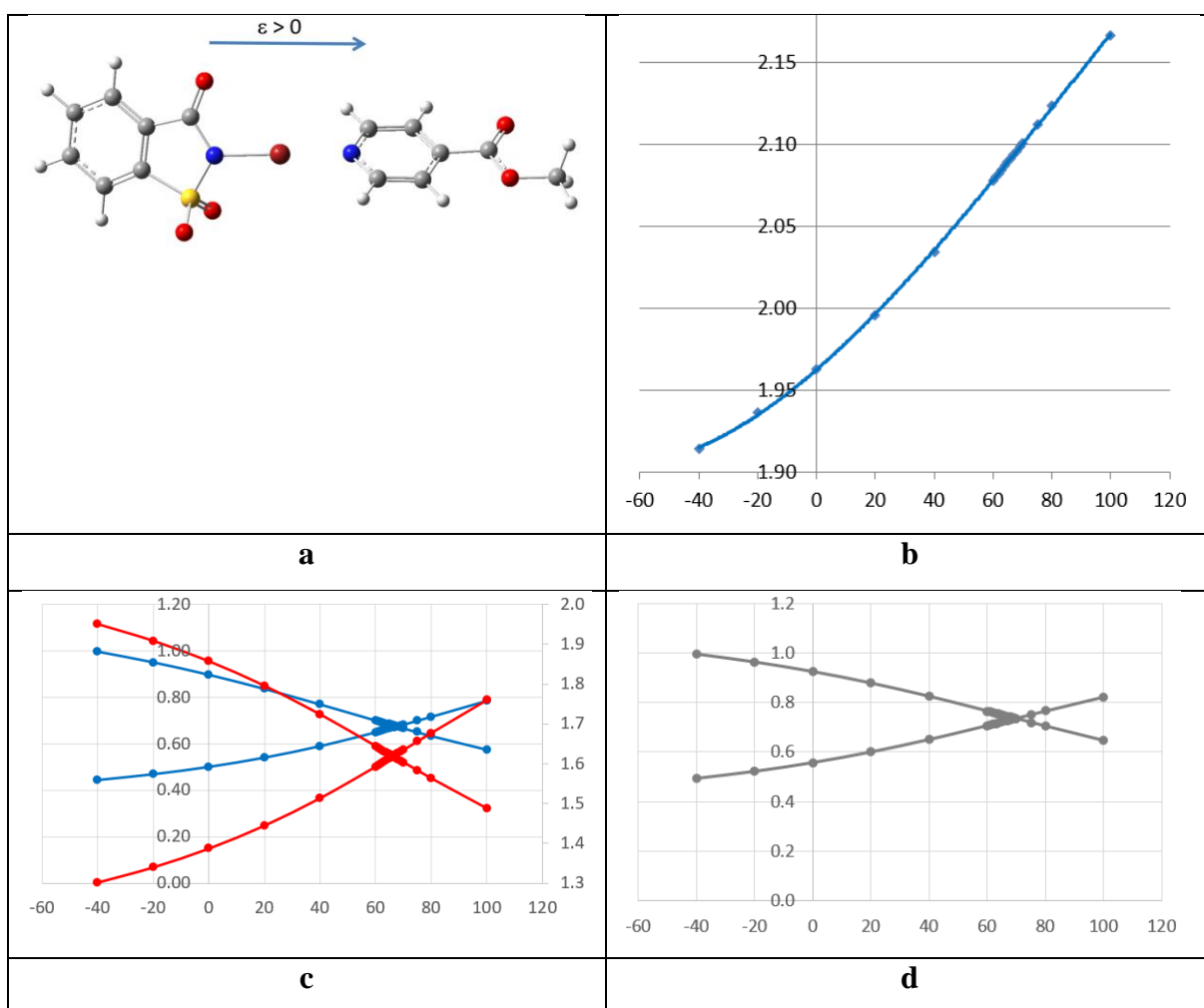


Figure S6. (a) NBrSac...PyCO₂Me adduct frozen at the experimental geometry (H atoms normalized at standard neutron distances) except for the Br-atom position, which has been optimized upon the application of an external electric field ϵ ranging $-40 < \epsilon < 100$ ($\times 10^{-4}$ a.u.), (b) $d(\text{N}_{\text{Sac}} \cdots \text{Br})$ (Å) vs ϵ ($\times 10^{-4}$ a.u.), the depicted fitting function is $d(\text{N}_{\text{Sac}} \cdots \text{Br}) = -3 \cdot 10^{-8} \cdot \epsilon^3 + 8 \cdot 10^{-6} \cdot \epsilon^2 + 1.6 \cdot 10^{-3} \cdot \epsilon + 1.9624$ (correlation factor $R^2 = 0.9999$). The corresponding ϵ vs $d(\text{N}_{\text{Sac}} \cdots \text{Br})$ curve leads to the fitting function $\epsilon = 5152.5 \cdot d^3 - 32356.4 \cdot d^2 + 68156.9 \cdot d - 48085.7$ (correlation factor $R^2 = 0.99999$), (c) ρ (blue curves and left scale in $\text{e}\text{\AA}^{-3}$) and $|V|/G$ (red curves and right scale dimensionless) at $\text{N}_{\text{Sac}} \cdots \text{Br}/\text{Br} \cdots \text{N}_{\text{Py}}$ BCPs (decreasing/increasing curves), and (d) DI vs ϵ for $\text{N}_{\text{Sac}} \cdots \text{Br}/\text{Br} \cdots \text{N}_{\text{Py}}$ interactions (decreasing/increasing curves). In (c) and (d), depicted curves are plotted for guiding eyes.

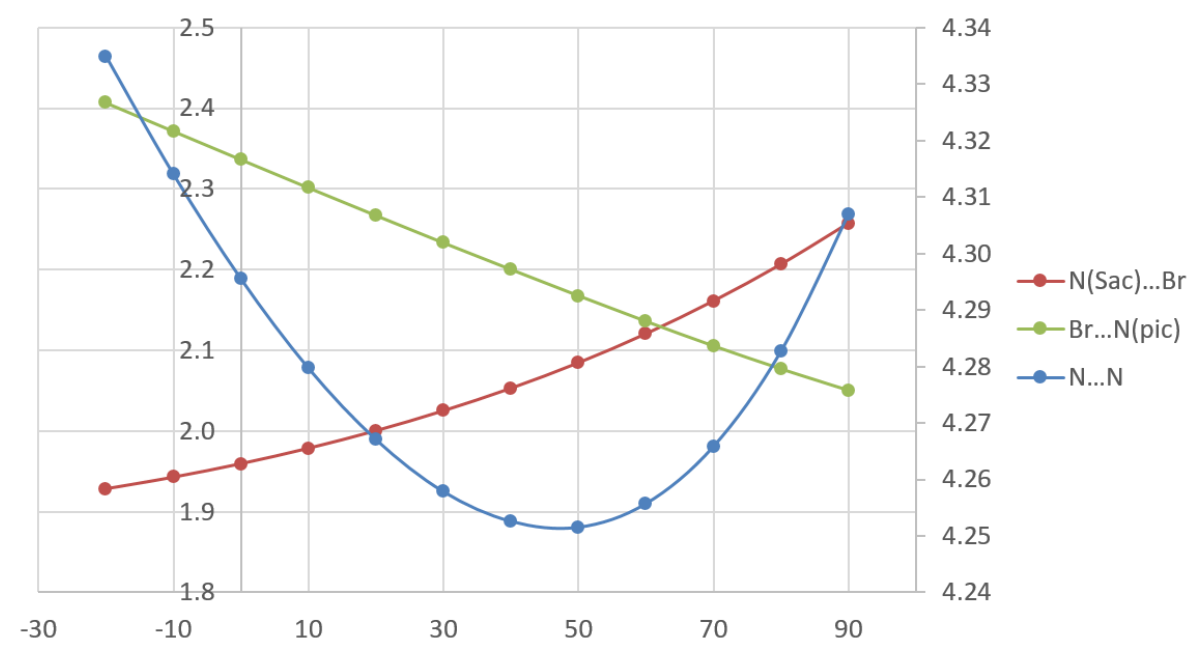


Figure S7. Distances (Å) $N_{\text{Sac}} \cdots \text{Br}$ and $\text{Br} \cdots N_{\text{Py}}$ (left scale), and $N_{\text{Sac}} \cdots N_{\text{Py}}$ (right scale), in the $N\text{BrSac} \cdots \text{PyMe}$ adduct as a function of the applied electric field ϵ ($\times 10^{-4}$ a.u.). Geometrical optimizations have been done for all atoms in the adduct. Depicted curves are plotted for guiding eyes.

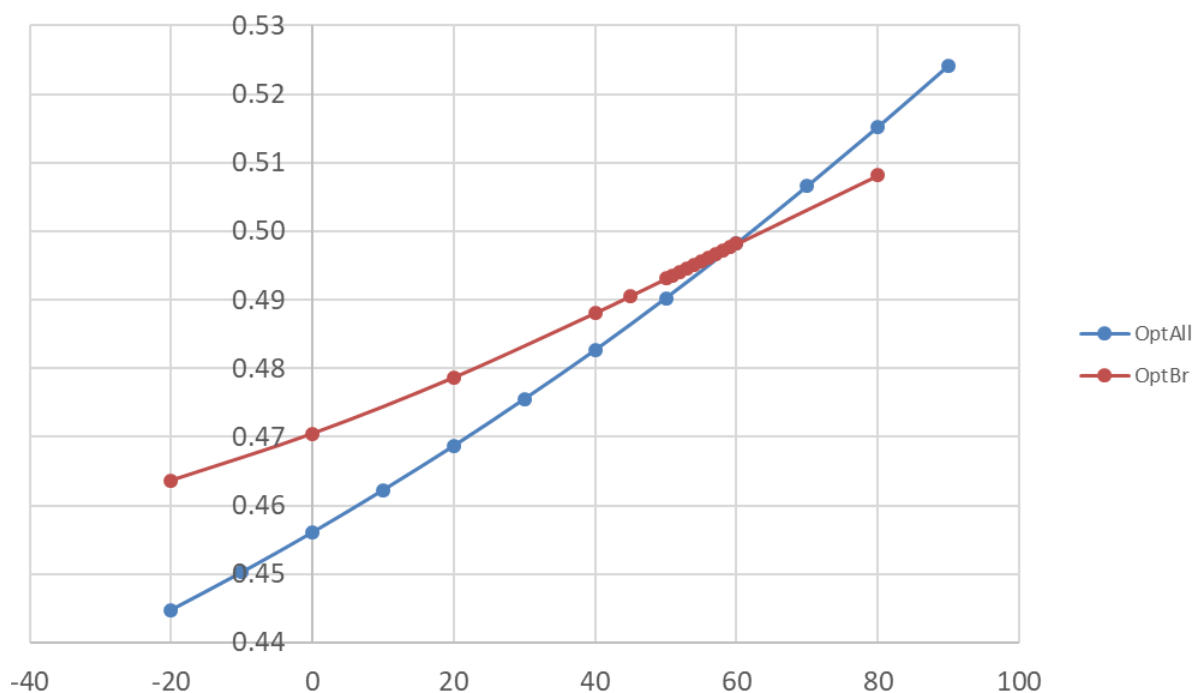


Figure S8. Normalized distance $N_{\text{Sac}}\cdots\text{Br}/N_{\text{Sac}}\cdots N_{\text{Py}}$ in the $\text{NBrSac}\cdots\text{PyMe}$ adduct as a function of the electric field ϵ ($\times 10^{-4}$ a.u.). Geometrical optimizations for the Br-atom only and for all atoms correspond respectively to red and blue data. Depicted curves are plotted for guiding eyes in their comparison. Due to the almost linear arrangement $N_{\text{Sac}}\cdots\text{Br}\cdots N_{\text{Py}}$ in the $\text{NBrSac}\cdots\text{PyMe}$ adduct, the behavior of the normalized distance as a function of ϵ at the acceptor side $\text{Br}\cdots N_{\text{Py}}/N_{\text{Sac}}\cdots N_{\text{Py}}$ shows a comparison between partial and full geometrical optimization that is very close to that observed at the donor side.

Table S1. Structural, topological and energetic properties at BCP's in $N_{Sac} \cdots Br / Br \cdots N'_{Py}$ regions of $NBrSac \cdots PyCN$ as a function of the applied electric field ε ($\times 10^4$ a.u.) ($\varepsilon = 0$ corresponds to the geometry where the halogen atom position was optimized while keeping frozen the rest of the atoms at the experimental geometry): distances $N_{Sac} \cdots Br / Br \cdots N'_{Py}$, electron density ρ ($e/\text{\AA}^3$), laplacian of the electron density $\nabla^2 \rho$ ($e/\text{\AA}^5$), electron kinetic (G), potential (V) and total ($H = G+V$) energy densities (a.u.), ratio ($|V|/G$) (dimensionless) and delocalization index (DI) (dimensionless).

ε	$N_{Sac} \cdots Br / Br \cdots N'_{Py}$	$Q(Br)$	ρ	$\nabla^2 \rho$	G	V	H	$ V /G$	DI
-60	1.877/2.347	0.308	1.074/0.391	-0.046/3.177	0.099/0.043	-0.199/-0.053	-0.100/-0.010	2.005/1.230	1.052/0.447
-40	1.890/2.333	0.305	1.043/0.404	0.182/3.126	0.096/0.043	-0.190/-0.054	-0.094/-0.011	1.980/1.253	1.031/0.459
-20	1.908/2.316	0.303	1.003/0.423	0.465/3.059	0.092/0.044	-0.179/-0.057	-0.087/-0.013	1.948/1.283	1.004/0.480
0	1.931/2.293	0.301	0.955/0.448	0.790/2.977	0.087/0.045	-0.167/-0.060	-0.079/-0.015	1.906/1.321	0.971/0.509
20	1.959/2.264	0.298	0.899/0.480	1.152/2.872	0.082/0.047	-0.152/-0.065	-0.070/-0.017	1.854/1.370	0.930/0.546
25	1.968/2.256	0.297	0.883/0.490	1.248/2.841	0.080/0.048	-0.148/-0.066	-0.067/-0.018	1.839/1.384	0.919/0.557
40	1.995/2.228	0.295	0.833/0.522	1.541/2.732	0.076/0.050	-0.135/-0.071	-0.060/-0.021	1.789/1.431	0.880/0.592
60	2.039/2.185	0.291	0.759/0.576	1.931/2.537	0.069/0.053	-0.118/-0.080	-0.049/-0.027	1.711/1.506	0.821/0.647
75	2.076/2.148	0.289	0.701/0.624	2.203/2.342	0.064/0.057	-0.106/-0.089	-0.042/-0.032	1.645/1.571	0.772/0.694
76	2.078/2.145	0.289	0.697/0.628	2.220/2.327	0.064/0.057	-0.105/-0.090	-0.041/-0.033	1.641/1.576	0.769/0.697
77	2.081/2.143	0.289	0.693/0.631	2.237/2.312	0.064/0.057	-0.104/-0.090	-0.041/-0.033	1.636/1.580	0.765/0.700
78	2.083/2.140	0.289	0.690/0.635	2.253/2.297	0.064/0.057	-0.104/-0.091	-0.040/-0.034	1.632/1.585	0.762/0.703
79	2.086/2.137	0.289	0.686/0.638	2.270/2.281	0.063/0.058	-0.103/-0.092	-0.040/-0.034	1.627/1.590	0.759/0.706
80	2.089/2.135	0.289	0.682/0.642	2.286/2.266	0.063/0.058	-0.102/-0.092	-0.039/-0.034	1.623/1.594	0.755/0.710
81	2.091/2.132	0.289	0.678/0.646	2.302/2.250	0.063/0.058	-0.101/-0.093	-0.039/-0.035	1.618/1.599	0.752/0.713

82	2.094/2.130	0.289	0.674/0.649	2.318/2.234	0.062/0.058	-0.101/-0.094	-0.038/-0.035	1.614/1.603	0.748/0.716
83	2.096/2.127	0.289	0.671/0.653	2.334/2.218	0.062/0.059	-0.100/-0.094	-0.038/-0.036	1.609/1.608	0.745/0.719
84	2.099/2.124	0.289	0.667/0.656	2.350/2.201	0.062/0.059	-0.099/-0.095	-0.037/-0.036	1.605/1.613	0.742/0.723
85	2.101/2.122	0.289	0.663/0.660	2.365/2.185	0.061/0.059	-0.098/-0.096	-0.037/-0.037	1.600/1.617	0.738/0.726
86	2.104/2.119	0.289	0.659/0.664	2.380/2.168	0.061/0.060	-0.098/-0.097	-0.036/-0.037	1.596/1.622	0.735/0.729
87	2.107/2.117	0.289	0.656/0.667	2.395/2.151	0.061/0.060	-0.097/-0.097	-0.036/-0.037	1.591/1.627	0.731/0.732
88	2.109/2.114	0.289	0.652/0.671	2.410/2.133	0.061/0.060	-0.096/-0.098	-0.036/-0.038	1.587/1.632	0.728/0.736
89	2.112/2.112	0.289	0.648/0.675	2.425/2.116	0.060/0.060	-0.095/-0.099	-0.035/-0.038	1.582/1.636	0.725/0.739
90	2.114/2.109	0.289	0.645/0.679	2.439/2.098	0.060/0.061	-0.095/-0.099	-0.035/-0.039	1.578/1.641	0.721/0.742
95	2.127/2.096	0.289	0.627/0.698	2.508/2.007	0.059/0.062	-0.091/-0.103	-0.033/-0.041	1.556/1.664	0.704/0.758
100	2.140/2.084	0.290	0.610/0.716	2.572/1.911	0.057/0.063	-0.088/-0.107	-0.031/-0.044	1.534/1.688	0.688/0.775
110	2.164/2.059	0.291	0.578/0.754	2.684/1.711	0.055/0.066	-0.082/-0.115	-0.027/-0.049	1.493/1.733	0.656/0.805
120	2.186/2.037	0.293	0.549/0.791	2.779/1.501	0.053/0.069	-0.077/-0.123	-0.024/-0.054	1.456/1.775	0.626/0.834
130	2.207/2.016	0.296	0.524/0.826	2.858/1.286	0.051/0.072	-0.073/-0.131	-0.022/-0.059	1.421/1.815	0.599/0.861

Table S2. Structural, topological and energetic properties at BCP's in $N_{Sac} \cdots Br / Br \cdots N_{Py}$ regions of $NBrSac \cdots PyCF_3$ as a function of the applied electric field ε ($\times 10^4$ a.u.) ($\varepsilon = 0$ corresponds to the geometry where the halogen atom position was optimized while keeping frozen the rest of the atoms at the experimental geometry): distances $N_{Sac} \cdots Br / Br \cdots N_{Py}$, electron density ρ ($e/\text{\AA}^3$), laplacian of the electron density $\nabla^2 \rho$ ($e/\text{\AA}^5$), electron kinetic (G), potential (V) and total ($H = G + V$) energy densities (a.u.), ratio ($|V|/G$) (dimensionless) and delocalization index (DI) (dimensionless).

ε	$N_{Sac} \cdots Br / Br \cdots N_{Py}$	Q(Br)	ρ	$\nabla^2 \rho$	G	V	H	$ V /G$	DI
-40	1.892/2.310	0.302	1.038/0.425	0.276/3.166	0.096/0.045	-0.190/-0.058	-0.093/-0.013	1.970/1.278	1.022/0.472
-20	1.911/2.291	0.303	0.996/0.446	0.577/3.089	0.092/0.046	-0.178/-0.061	-0.086/-0.014	1.935/1.311	0.994/0.497
0	1.934/2.267	0.302	0.947/0.473	0.909/2.994	0.087/0.048	-0.165/-0.065	-0.078/-0.017	1.892/1.352	0.959/0.529
20	1.963/2.238	0.300	0.890/0.507	1.269/2.874	0.082/0.050	-0.150/-0.070	-0.069/-0.020	1.839/1.402	0.918/0.567
40	1.998/2.203	0.297	0.826/0.550	1.645/2.716	0.076/0.053	-0.135/-0.077	-0.059/-0.024	1.775/1.464	0.869/0.613
60	2.040/2.161	0.295	0.756/0.604	2.016/2.503	0.070/0.056	-0.119/-0.086	-0.049/-0.030	1.700/1.537	0.812/0.666
75	2.073/2.127	0.294	0.703/0.650	2.272/2.298	0.065/0.059	-0.107/-0.095	-0.042/-0.035	1.639/1.598	0.767/0.709
76	2.076/2.125	0.294	0.699/0.654	2.287/2.283	0.065/0.060	-0.106/-0.095	-0.041/-0.036	1.635/1.602	0.764/0.712
77	2.078/2.123	0.294	0.696/0.657	2.303/2.268	0.065/0.060	-0.106/-0.096	-0.041/-0.036	1.631/1.607	0.761/0.715
78	2.080/2.121	0.294	0.692/0.660	2.319/2.253	0.065/0.060	-0.105/-0.097	-0.040/-0.037	1.627/1.611	0.757/0.718
79	2.083/2.118	0.294	0.689/0.664	2.334/2.237	0.064/0.060	-0.104/-0.097	-0.040/-0.037	1.623/1.615	0.754/0.721
80	2.085/2.116	0.294	0.685/0.667	2.350/2.221	0.064/0.061	-0.104/-0.098	-0.040/-0.037	1.619/1.619	0.751/0.724
81	2.087/2.114	0.294	0.682/0.670	2.365/2.205	0.064/0.061	-0.103/-0.099	-0.039/-0.038	1.615/1.624	0.748/0.727
82	2.090/2.111	0.294	0.678/0.674	2.380/2.189	0.063/0.061	-0.102/-0.099	-0.039/-0.038	1.611/1.628	0.745/0.730

83	2.092/2.109	0.294	0.675/0.677	2.395/2.172	0.063/0.061	-0.101/-0.100	-0.038/-0.039	1.607/1.632	0.742/0.733
84	2.094/2.107	0.294	0.671/0.680	2.410/2.156	0.063/0.062	-0.101/-0.101	-0.038/-0.039	1.602/1.636	0.739/0.736
85	2.097/2.104	0.294	0.668/0.684	2.424/2.139	0.063/0.062	-0.100/-0.101	-0.037/-0.040	1.598/1.641	0.736/0.739
90	2.108/2.093	0.294	0.651/0.701	2.494/2.053	0.061/0.063	-0.097/-0.105	-0.035/-0.042	1.578/1.662	0.720/0.754
95	2.120/2.081	0.295	0.635/0.719	2.560/1.964	0.060/0.064	-0.094/-0.108	-0.034/-0.044	1.558/1.684	0.705/0.769
100	2.131/2.070	0.295	0.619/0.736	2.621/1.871	0.059/0.066	-0.091/-0.112	-0.032/-0.046	1.538/1.705	0.690/0.783

Table S3. Structural, topological and energetic properties at BCP's in $N_{\text{Sac}}\cdots\text{Br}/\text{Br}\cdots N_{\text{Py}}$ regions of $\text{NBrSac}\cdots\text{PyCO}_2\text{Me}$ as a function of the applied electric field ε ($\times 10^4$ a.u.) ($\varepsilon = 0$ corresponds to the geometry where the halogen atom position was optimized while keeping frozen the rest of the atoms at the experimental geometry): distances $N_{\text{Sac}}\cdots\text{Br}/\text{Br}\cdots N_{\text{Py}}$, electron density ρ ($\text{e}/\text{\AA}^3$), laplacian of the electron density $\nabla^2\rho$ ($\text{e}/\text{\AA}^5$), electron kinetic (G), potential (V) and total ($H = G + V$) energy densities (a.u.), ratio ($|V|/G$) (dimensionless) and delocalization index (DI) (dimensionless).

ε	$N_{\text{Sac}}\cdots\text{Br}/\text{Br}\cdots N_{\text{Py}}$	Q(Br)	ρ	$\nabla^2\rho$	G	V	H	$ V /G$	DI
-40	1.914/2.293	0.289	0.996/0.443	0.425/3.153	0.090/0.047	-0.175/-0.061	-0.085/-0.014	1.951/1.302	0.996/0.492
-20	1.936/2.271	0.288	0.950/0.468	0.752/3.063	0.085/0.048	-0.163/-0.064	-0.078/-0.016	1.909/1.340	0.964/0.521
0	1.963/2.243	0.286	0.897/0.500	1.107/2.949	0.080/0.050	-0.150/-0.069	-0.069/-0.019	1.857/1.387	0.925/0.556
20	1.996/2.210	0.284	0.836/0.540	1.480/2.801	0.075/0.052	-0.135/-0.076	-0.060/-0.023	1.796/1.444	0.878/0.600
40	2.034/2.171	0.282	0.770/0.590	1.852/2.604	0.069/0.056	-0.120/-0.084	-0.050/-0.028	1.723/1.513	0.824/0.650
60	2.078/2.128	0.281	0.701/0.649	2.195/2.342	0.064/0.060	-0.105/-0.095	-0.041/-0.035	1.644/1.592	0.765/0.707
61	2.080/2.126	0.281	0.697/0.653	2.211/2.327	0.064/0.060	-0.104/-0.095	-0.041/-0.036	1.640/1.596	0.762/0.710
62	2.082/2.123	0.281	0.694/0.656	2.227/2.312	0.063/0.060	-0.104/-0.096	-0.040/-0.036	1.636/1.601	0.759/0.713
63	2.085/2.121	0.281	0.690/0.659	2.243/2.296	0.063/0.060	-0.103/-0.097	-0.040/-0.036	1.631/1.605	0.756/0.715
64	2.087/2.119	0.281	0.687/0.662	2.258/2.281	0.063/0.061	-0.102/-0.097	-0.039/-0.037	1.627/1.609	0.753/0.718
65	2.089/2.117	0.281	0.683/0.666	2.274/2.265	0.063/0.061	-0.102/-0.098	-0.039/-0.037	1.623/1.613	0.750/0.721
66	2.092/2.114	0.281	0.680/0.669	2.289/2.249	0.062/0.061	-0.101/-0.099	-0.039/-0.038	1.619/1.617	0.747/0.724
67	2.094/2.112	0.281	0.677/0.672	2.304/2.233	0.062/0.061	-0.100/-0.099	-0.038/-0.038	1.615/1.622	0.744/0.727
68	2.096/2.110	0.281	0.673/0.675	2.319/2.217	0.062/0.061	-0.100/-0.100	-0.038/-0.038	1.611/1.626	0.741/0.730

69	2.098/2.107	0.281	0.670/0.679	2.333/2.200	0.062/0.062	-0.099/-0.101	-0.037/-0.039	1.607/1.630	0.738/0.733
70	2.101/2.105	0.281	0.667/0.682	2.348/2.184	0.061/0.062	-0.098/-0.101	-0.037/-0.039	1.603/1.634	0.735/0.736
75	2.112/2.094	0.282	0.650/0.699	2.418/2.098	0.060/0.063	-0.095/-0.105	-0.035/-0.041	1.582/1.655	0.719/0.751
80	2.123/2.082	0.282	0.634/0.716	2.484/2.008	0.059/0.064	-0.092/-0.108	-0.033/-0.044	1.562/1.677	0.704/0.765
100	2.167/2.039	0.286	0.575/0.785	2.707/1.618	0.055/0.070	-0.081/-0.123	-0.027/-0.053	1.487/1.759	0.645/0.822

Table S4. Structural, topological and energetic properties at BCP's in N_{Sac}•••Br /Br•••NⁱPy regions of NBrSac•••PyMe as a function of the applied electric field ε ($\times 10^4$ a.u.) ($\varepsilon = 0$ corresponds to the geometry where the halogen atom position was optimized while keeping frozen the rest of the atoms at the experimental geometry): distances N_{Sac}•••Br/ Br•••NⁱPy, electron density ρ ($e/\text{\AA}^3$), laplacian of the electron density $\nabla^2\rho$ ($e/\text{\AA}^5$), electron kinetic (G), potential (V) and total (H= G+V) energy densities (a.u.), ratio ($|V|/G$) (dimensionless) and delocalization index (DI) (dimensionless).

ε	N _{Sac} •••Br/ Br•••N ⁱ Py	Q(Br)	ρ	$\nabla^2\rho$	G	V	H	$ V /G$	DI
-40	1.910/2.261	0.303	0.996/0.475	0.625/3.147	0.093/0.050	-0.179/-0.067	-0.086/-0.017	1.930/1.341	0.986/0.523
-20	1.934/2.237	0.302	0.947/0.503	0.958/3.036	0.088/0.051	-0.166/-0.071	-0.078/-0.020	1.887/1.383	0.951/0.555
0	1.962/2.209	0.300	0.890/0.538	1.317/2.896	0.082/0.053	-0.151/-0.076	-0.069/-0.023	1.834/1.435	0.910/0.593
20	1.997/2.175	0.297	0.827/0.582	1.690/2.715	0.077/0.056	-0.136/-0.084	-0.059/-0.028	1.771/1.496	0.861/0.638
40	2.036/2.135	0.295	0.760/0.636	2.054/2.479	0.071/0.060	-0.120/-0.093	-0.050/-0.034	1.699/1.568	0.807/0.689
45	2.046/2.125	0.295	0.743/0.651	2.140/2.410	0.069/0.061	-0.117/-0.096	-0.047/-0.036	1.680/1.587	0.792/0.703
50	2.057/2.114	0.295	0.726/0.666	2.223/2.337	0.068/0.062	-0.113/-0.099	-0.045/-0.037	1.661/1.607	0.778/0.717
51	2.059/2.112	0.295	0.723/0.669	2.240/2.322	0.068/0.062	-0.112/-0.100	-0.045/-0.038	1.657/1.610	0.775/0.720
52	2.061/2.110	0.295	0.720/0.672	2.256/2.307	0.068/0.062	-0.112/-0.100	-0.044/-0.038	1.653/1.614	0.772/0.723
53	2.063/2.108	0.295	0.716/0.675	2.272/2.291	0.067/0.062	-0.111/-0.101	-0.044/-0.039	1.650/1.618	0.769/0.725
54	2.065/2.106	0.295	0.713/0.678	2.288/2.276	0.067/0.063	-0.110/-0.101	-0.043/-0.039	1.646/1.622	0.766/0.728
55	2.067/2.104	0.295	0.710/0.681	2.304/2.260	0.067/0.063	-0.110/-0.102	-0.043/-0.039	1.642/1.626	0.763/0.731
56	2.069/2.102	0.295	0.707/0.684	2.319/2.244	0.066/0.063	-0.109/-0.103	-0.042/-0.040	1.638/1.630	0.760/0.734
57	2.072/2.100	0.295	0.703/0.688	2.335/2.228	0.066/0.063	-0.108/-0.103	-0.042/-0.040	1.634/1.634	0.758/0.737

58	2.074/2.097	0.295	0.700/0.691	2.350/2.212	0.066/0.063	-0.107/-0.104	-0.042/-0.040	1.630/1.638	0.755/0.739
59	2.076/2.095	0.295	0.697/0.694	2.365/2.195	0.066/0.064	-0.107/-0.105	-0.041/-0.041	1.626/1.642	0.752/0.742
60	2.078/2.093	0.295	0.693/0.697	2.380/2.179	0.065/0.064	-0.106/-0.105	-0.041/-0.041	1.623/1.646	0.749/0.745
80	2.120/2.051	0.296	0.632/0.763	2.650/1.821	0.061/0.069	-0.094/-0.119	-0.033/-0.050	1.547/1.726	0.692/0.800
100	2.158/2.013	0.299	0.579/0.828	2.860/1.426	0.057/0.074	-0.084/-0.133	-0.027/-0.059	1.479/1.800	0.639/0.851

Table S5. Structural properties of NBrSac•••PyMe as a function of the applied electric field ε ($\times 10^{-4}$ a.u.) resulting from full geometrical optimization. The torsion angle C(SO₂)-C(CO)-N-Br is used as a measure of the planarity of the adduct.

ε	N _{Sac} •••Br (Å)	Br•••N ^{Py} (Å)	N _{Sac} •••N ^{Py} (Å)	N _{Sac} •••Br / N _{Sac} •••N ^{Py}	Br•••N ^{Py} / N _{Sac} •••N ^{Py}	C(SO ₂)-C(CO)-N-Br (°)
-20	1.928	2.407	4.335	0.445	0.555	-177.60
-10	1.943	2.371	4.314	0.450	0.550	-179.42
0	1.959	2.336	4.296	0.456	0.544	179.93
10	1.978	2.301	4.280	0.462	0.538	179.54
20	2.000	2.267	4.267	0.469	0.531	179.68
30	2.025	2.233	4.258	0.476	0.524	179.81
40	2.053	2.200	4.253	0.483	0.517	179.81
50	2.084	2.167	4.252	0.490	0.510	179.97
60	2.120	2.136	4.256	0.498	0.502	179.94
70	2.161	2.105	4.266	0.507	0.494	179.90
80	2.206	2.077	4.283	0.515	0.485	179.90
90	2.257	2.050	4.307	0.524	0.476	179.35

